Origins of directionality in snapping shrimp sounds and its potential applications

Mandar Chitre, Koay Teong Beng, John Potter

Acoustic Research Laboratory, Tropical Marine Science Institute
National University of Singapore, 12a Kent Ridge Road, Singapore 119223
mandar@arl.nus.edu.sg, koay@arl.nus.edu.sg, johnp@arl.nus.edu.sg

ABSTRACT

Snapping shrimp (genera *Alpheus, Synalpheus & Penaeus*) sounds are known to dominate high frequency ambient noise in warm shallow waters with a peak-to-peak source levels of up to 190 dB re 1uPa @ 1m. It has been previously shown that these loud sounds are primarily due to the collapse of cavitation bubbles resulting from the ejection of a high-speed jet of water generated by the high-speed closure of the snapping shrimp claw. As the cavitation bubble is small, it is expected to behave as an omni-directional source. However, since snapping shrimp live on or very close to the sea bed, the source and the bottom reflection of the source form a quasi-dipole. The interference between the direct arrival from the source and the closely-spaced bottom-reflected arrival creates directionality. The observed directionality of the snapping shrimp sound is a function of the bottom parameters, because of their influence on the reflected component of the quasi-dipole. Since the shrimp are distributed over a wide portion of the seabed, the directionality resulting from many different arrival angles may be used for geoacoustic inversion at a single receiving location, yielding estimates of superficial bottom parameters such as sound speed from a single receiver station deployment and without introducing deterministic sources.

The Acoustic Research Laboratory (ARL) at the Tropical Marine Science Institute of Singapore has developed a compact, high-bandwidth, 3-dimensional acoustic array that can localise these sources in time and space. Data from experimental deployments of this system provides evidence for the directionality of snapping shrimp sound.

I. INTRODUCTION

Snapping shrimp (genera Alpheus & Synalpheus) sounds are known to dominate high frequency ambient noise in warm shallow waters with a peak-to-peak source levels of up to 190 dB re 1uPa @ 1m [1]. It has been previously shown that these loud sounds are primarily due to the collapse of cavitation bubbles resulting from the ejection of a jet of water generated by the high-speed closure of the snapping shrimp claw [2]. As the cavitation bubble is small, it is expected to behave as an omni-directional source. However, since snapping shrimp live on or very close to the sea bed, the source and the bottom reflection of the source form a quasi-dipole. The interference between the direct arrival from the source and the closely-spaced bottom-reflected arrival creates directionality. The observed directionality of the snapping shrimp sound is a function of the bottom parameters, because of their influence on the reflected component of the quasi-dipole.

II. THEORETICAL MODEL

With certain simplifying assumptions, it is possible to model the interaction between the direct arrival and the bottom reflected arrival of the snapping shrimp sound (a snap).

Let us assume a snapping shrimp sitting on or near the seabed in water depth d. We observe the shrimp using a hydrophone placed at a horizontal distance R from the shrimp and at an angle of elevation Φ. Say, the bubble collapse (causing the snap) happens at a small distance δ above the seabed. This arrangement is illustrated in Fig. 1.

Let c be the speed of sound in water. Assuming the snap occurs at time 0, the direct arrival reaches the hydrophone at time t_1,

$$t_1 = \frac{1}{c}\sqrt{(h-\delta)^2 + R^2}$$

$$where\ h = R\tan\phi$$

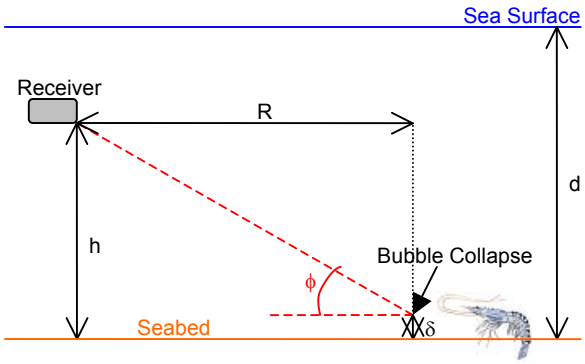

Fig. 1. Arrangement of snapping shrimp and receiver for theoretical model

By the method of images, the bottom reflected arrival reaches the hyrdophone at a slightly later time t_2,

$$t_2 = \frac{1}{c}\sqrt{(h+\delta)^2 + R^2}$$

Assuming δ is small as compared to R, d and h, the difference between the times of arrival can be approximated using the first order terms in the Taylor series expansion.

$$\Delta t = t_2 - t_1 \approx \frac{2\delta}{c}\sin\phi$$

If Δt is more than the width of the peak of the snap[a], the snap and the reflection do not interfere significantly and the two arrivals can be observed independently. If Δt is less than the peak width, the snap and the reflection interfere to yield a single observable snap with a different energy than the source snap.

Let the density of water be ρ. For a bottom with no absorption, speed of sound c_1 and density ρ_1, the reflection coefficient (V) is given by [3],

$$V = \frac{m\sin\phi - \sqrt{n^2 - \cos^2\phi}}{m\sin\phi + \sqrt{n^2 - \cos^2\phi}}$$

$$where \quad m = \rho_1/\rho, \quad n = c/c_1$$

For Φ above the critical angle, V is real and the reflected snap is an attenuated copy of the original snap.

For Φ less than the critical angle, V is complex with |V| = 1. The reflected snap is a phase rotated version of the original snap; the shape of the reflected snap may be significantly distorted when compared to the shape of the original snap.

III. NUMERICAL SIMULATION

Apart from special or limiting cases of Φ and δ, the general analysis of the theoretical model is difficult. A numerical simulation based on the model, aids in the understanding of the behaviour of the model for different values of Φ and δ.

An ideal snap (shown in Fig. 2) was modelled based on the average of a large number of observed snaps at different angles. The model consists of a small precursor at the time of closing of the claw, followed by a sharp snap produced by the collapse of the cavitation bubble. The time between the precursor and the bubble collapse varies substantially (up to 10x) between snaps samples from different geographical areas. This may be due to differences is jet speeds or bubble stability across different species of snapping shrimp. The collapse height, δ, may also be partly correlated to the time between the precursor and bubble collapse, as the bubble is likely to travel further from the seabed given a longer time before collapse.

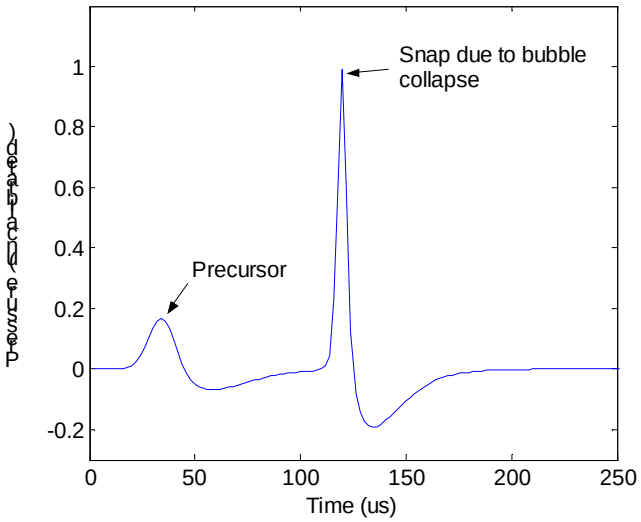

Fig. 2. A synthetic stereotypical model snap

The theoretical model was applied to the ideal snap to obtain snaps at different values of Φ and δ. A sample result from the theoretical model is shown in Fig. 3. The actual shape of the time series can vary substantially based on Φ and δ. For the sample shown here, the secondary snap peak is clearly visible but the secondary precursor

[a] The width of the peak is theoretically expected to be in the order of picoseconds [2]; however, due to the low pass filtering effect of the ocean and the limited sampling rate (and associated anti-aliasing filters), the observed peak width is usually around 5 μs (estimated at sampling rate of 0.5 MHz).

combines with the primary precursor, effectively broadening it.

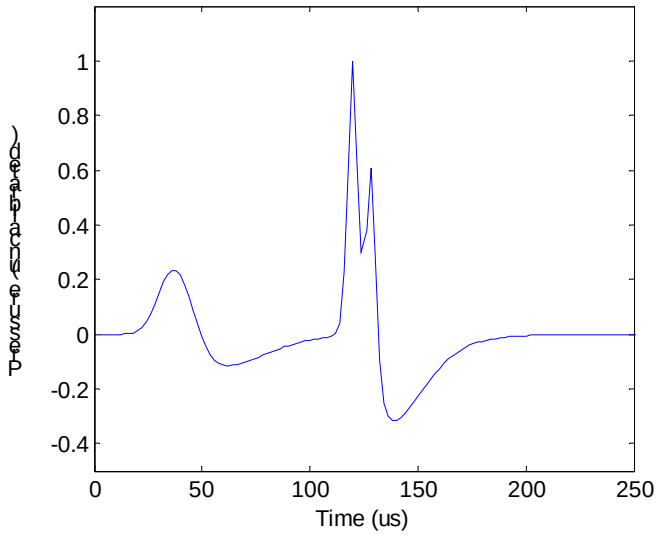

Fig. 3. Simulated snap with at Φ = 21°, δ = 1.5 cm, c_1 = 1600 m/s, ρ_1 = 1800 kg/m^3

The total energy in a snap observed at various angles, given a bubble collapse height and bottom parameters, was calculated using the numerical model. As seen in Fig. 4, the angle with the peak energy is relatively insensitive δ. However, the drop in observed energy at large angles as compared to the peak energy is sensitive to δ.

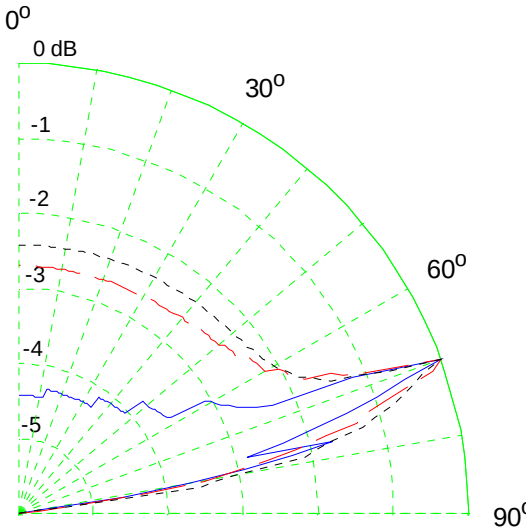

Fig. 4. Directionality of snap energy measured at δ = 1 (solid), 2 (dashed), 3 (dotted) cm with c_1 = 1600 m/s, ρ_1 = 1800 kg/m^3

Fig. 5 shows the directionality of the snap energy at different bottom sound speed. The angular position of the peak is sensitive to the sound speed.

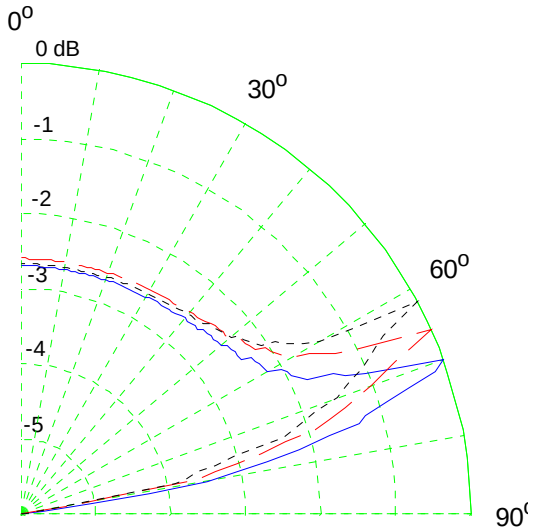

Fig. 5. Directionality of snap energy measured at c_1 = 1600 (solid), 1650 (dashed), 1700 (dotted) m/s with δ = 2 cm, ρ_1 = 1800 kg/m^3

The peak occurs at the critical angle for small values of δ. However, for large values of δ, the peak broadens and has its lower cut-off angle at the critical angle. An example of such a broadened peak is seen in Fig. 6.

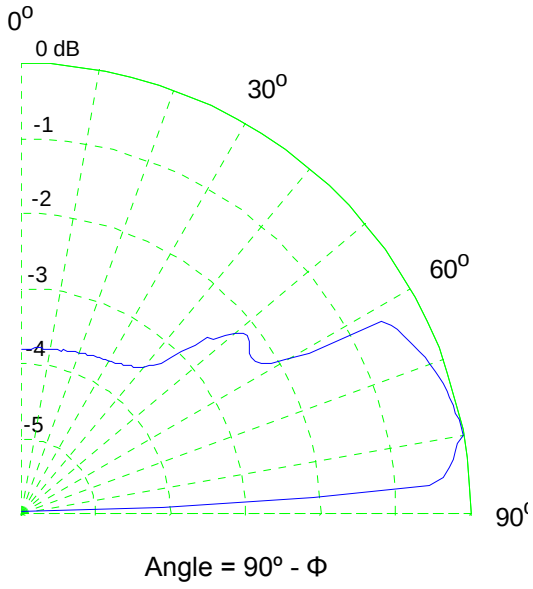

Fig. 6. Directionality of snap energy measured at δ = 10 cm, c_1 = 1700 m/s, ρ_1 = 1800 kg/m^3

It turns out, however, that the directionality of the snap energy is not very sensitive to the bottom density.

IV. EXPERIMENTAL VALIDATION

Snapping shrimp sound recordings from various experimental deployments provide evidence for the validity of the theoretical models described earlier in this paper. The experimental setup, observed data and analysis from one such deployment is presented in this section.

A. Experimental Setup

An experimental setup consists of a receiver suspended at a height h above the seabed in a known water depth d, as shown in Fig. 1. The receiver consists of an array of hydrophones fixed at the corners of a tetrahedral (each side is 1.2m). Assuming a locally flat bathymetry, the receiver can compute the direction (elevation, azimuth) and range for each snap arriving at the receiver.

Correcting for spreading loss[b], the energy emitted by the snap in the direction of the receiver can be estimated. A plot of direction of arrival against estimated source energy from the experimental results is shown in Fig. 7. The average source energy shown in the plot is estimated using a 200μs window around the peak.

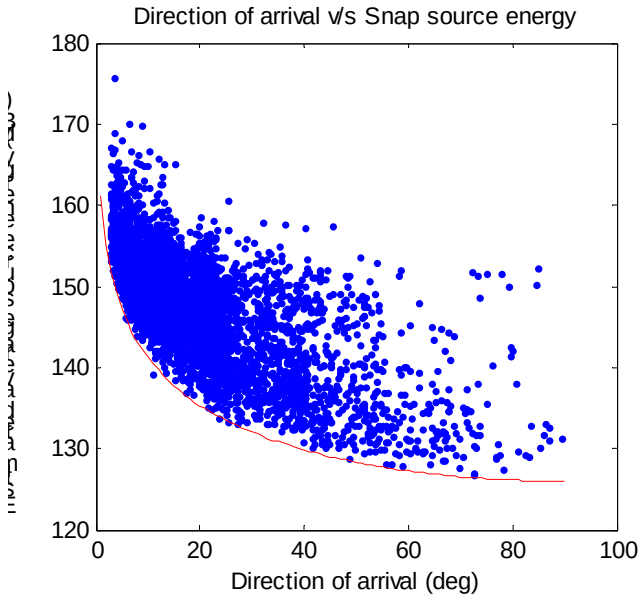

Fig. 7. 6901 individual snaps detected from a 4 minute recording as a function of direction of arrival

[b] Attenuation is ignored as the range of interest for snap detection is small, approximately 100 m

The peak source energy is, on an average, 14dB higher than the average source energy shown here. The red solid line shows the theoretical minimum detection curve (equations follow) fitted to the data.

$$E_0 = E_t + 20\log_{10}\left(\frac{h}{\sin\phi}\right)$$

$$where \quad E_t = 106 \quad (fitted)$$

$$and \quad h = 10 \quad (known)$$

The fitted value of 106 dB is quite reasonable for E_t, knowing that the measured background noise level in the acquired data was about 100 dB and the detection threshold was set to 6 dB above background noise.

The number of snapping shrimp at small angles is likely to be large. However, as the range at small angles is large, the SNR for snaps from these shrimp is low and hence only few or no snaps may be detected.

At large angles, the range is short and almost all snaps are likely to be detectable. However, the number of shrimp at these angles is likely to be small and hence only a few snaps from these angles may be detected.

At intermediate angles, where the range is short enough for good SNR and the angle is large enough that the number of shrimp is expected to be reasonable, most amount of data may be obtained. As long as the critical angle lies within this range, we may expect to be able to perform an experimental validation that a significant change (> 2 dB, based on the model) in observed snap energy occurs at the critical angle.

B. Observed Snaps

Fig. 8 shows observed snaps at different elevation angles and different (but unknown) bubble collapse height above the seabed.

Large values of Φ yield real values of V. The peak pressure in the reflected arrival is small as compared to the peak pressure in the direct arrival. Often the reflected arrival is lost in noise, unless the snap is quite close to the hydrophone.

As Φ reduces towards the critical angle, V becomes larger (and continues to be real). A snap with a double peak is often observed at such angles as seen in Fig. 8 (a). Δt is dependent on the angle as well as δ.

Below the critical angle, Δt is often too small to be able to differentiate between the direct and the reflected arrivals. With the phase rotated snap interfering with the direct arrival, the shape of the observed snap changes significantly. Close to the critical angle, secondary peaks are often observable (as seen in Fig. 8 (b)), but are much

smaller than the primary peak as the energy in the reflected snap is spread over a longer time due to the phase shift during total internal reflection.

As Φ reduces further, the phase shift causes the reflected snap to be more distorted, frequently resulting in snaps as seen in Fig. 8 (c). Sometimes, large negative pressure components are seen in such snaps, even though they are absent in the original snap. The shapes of these snaps vary significantly as the angle of observation and the bubble collapse height above the sea bottom change.

As Φ approaches zero, Δt approaches zero and the phase shift of the reflected snap approaches 180º. The reflected snap tends to cancel out and direct arrival, resulting in very little energy being radiated towards the hydrophone. At low Φ, the signal to noise ratio drops and the snaps become undetectable.

C. Distribution of Source Snap Energy

Angular windows with 5º width were used to get samples of snaps at given mean angles. These snaps were then used to empirically estimate the distribution of the source energy at the angle. The empirical distribution (empirical PDF) was estimated using a Gaussian-smoothed histogram (using the MATLAB ksdensity function).

At low angles, the samples contain a large number of snaps and hence yield higher precision estimates of the distribution. However, at very low angles, the accuracy of the angle estimate is low, the SNR is low and the constant depth bathymetry assumption is likely to be violated. At high angles, the samples contain too few snaps to allow precise estimates of distribution. Hence we only used mean angles between 5º and 56º in the estimation of the distribution.

As seen in Fig. 9 (a), at low angles a normal distribution in dB space yielded a good match to the observed data. However, at higher angles the observed distribution was clearly bimodal as seen in Fig. 9 (b) and (c). A weighted sum of two normal distributions in dB space yielded good match to the observed bimodal distribution.

Many different criteria for evaluating goodness of fit were tested – eg. χ^2 goodness of fit, KL divergence, least mean square error (MSE). The final criterion for fitting the parametric bimodal distribution to the observed data was the bimodal MSE. It was selected over the others because the others exhibit a bias in fit towards the low probability regions. The MSE criterion is more balanced and yields better overall fits to the empirical distribution.

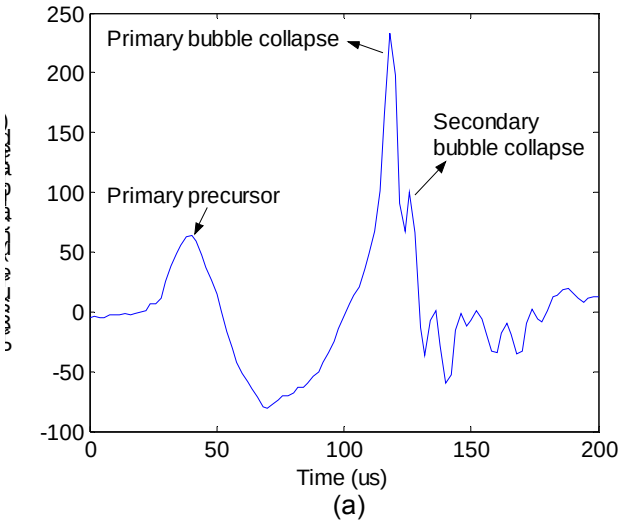

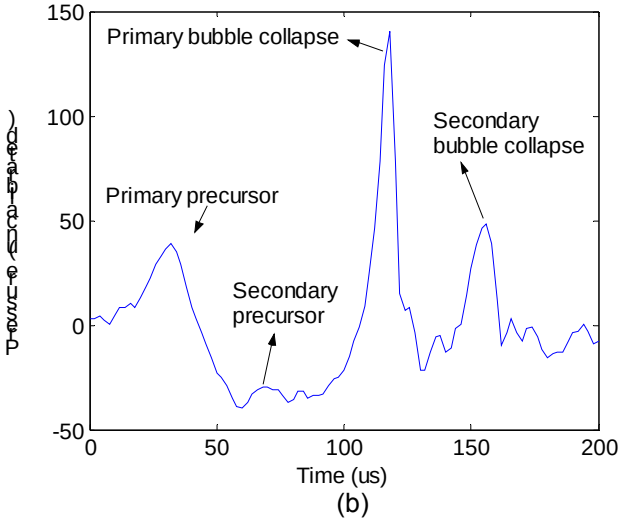

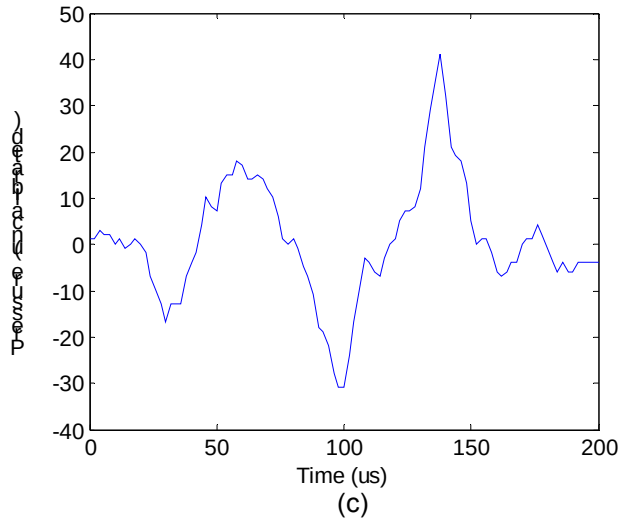

Fig. 8. Observed snaps at elevation angles of (a) 21.5º, (b) 15º and (c) 7.5º

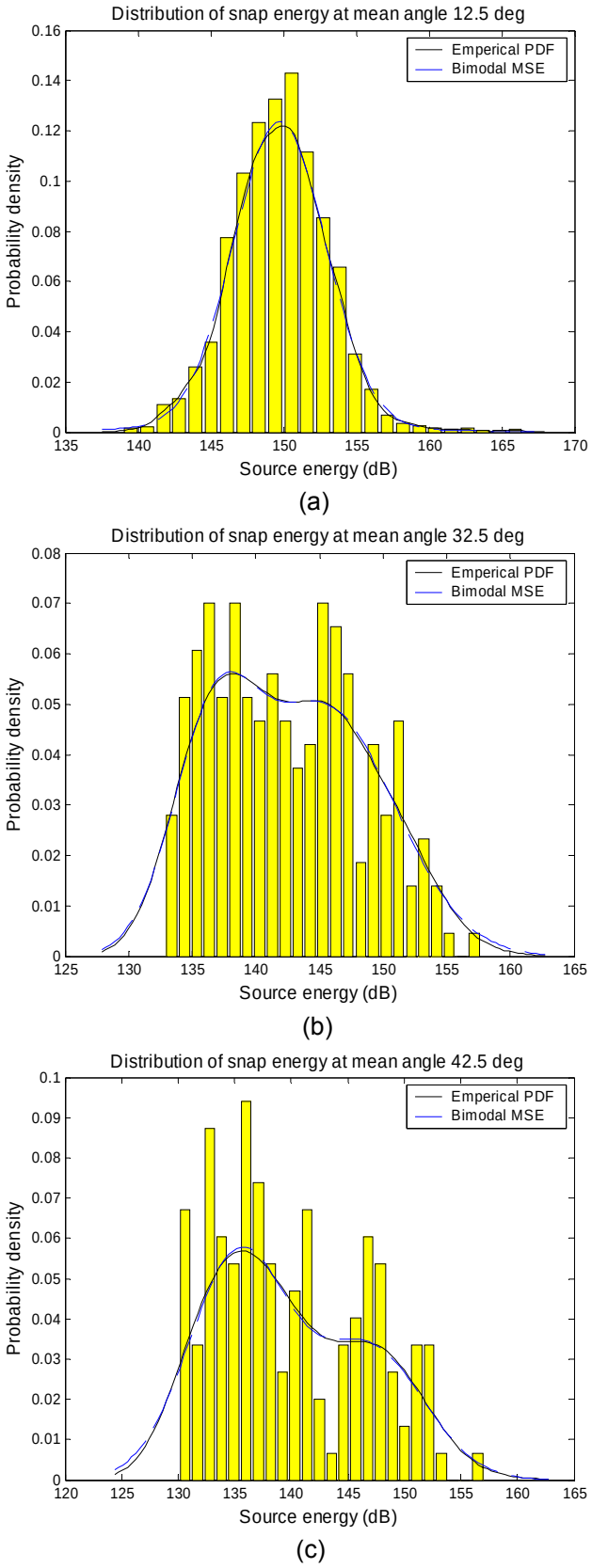

Fig. 9. Distribution of total snap energy at various angles of observation

D. Interpretation of the Bimodal Distribution

The bimodal distribution seems to comprise of two normal distributions in dB space. In linear space, this translates to a combination of two log-normal distributions.

It has been known for a while now that the snapping shrimp originated acoustic energy is log-normally distributed [4][5]. It was thought that the distribution may be either due to spatial clumping or due to temporal chorusing [6]. However, the observed log-normal distribution in this paper is based on the individual snap strengths rather than the mean energy and therefore cannot be explained by either of the hypothesis. It may be that the source snap strength may be log-normally distributed due to the distribution of the size of the snapping shrimp claw and its non-linear relation to the mechanism of the bubble formation and eventual collapse (which results in the loud snap).

The observed bimodality may indicate that there are two distinct species of snapping shrimp at the experimental site. The mean size of each species may be different, resulting in different mean snap strengths. This hypothesis is reasonable in light of the fact that Singapore waters (where this experiment was performed) is believed to house more than one species of snapping shrimp.

One of the component log-normal distribution hovers around a mean source energy of 145-150 dB at most angles. The other component distribution seems to have reducing mean source energy with increasing angle. This may indicate that the true mean source energy for this distribution is lower than the detection threshold and we are observing only the tail end of the distribution as explained in the next section.

If this hypothesis is correct, we would expect that the contribution from the second component distribution would increase as the detection threshold reduces (or the angle increases). This is indeed observed – the component contribution increases from about 20% to about 65% as the angle increases from 5º to 55º. As the contribution from the second component increases at higher angles, the observed distribution seems to be slightly skewed positively, as would be expected from this model.

E. Clipped Probability Distribution

When a probability distribution is non-uniformly sampled, the apparent distribution is likely to have different statistical characteristics than the original distribution.

If a normal distribution is sampled only above a given threshold, it may appear similar to a normal distribution with a higher mean and lower variance

as shown in Fig. 10. As the threshold is lowered, the mean of the apparent distribution may appear to reduce as well.

This effect may be contributing to the observation that one of the modes of the fitted bimodal distribution seems to have a mean that reduces with increased elevation angle (and hence reduced threshold).

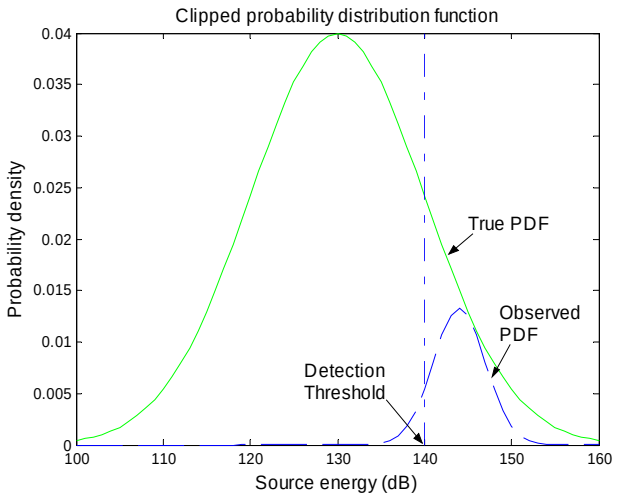

Fig. 10. Clipped observed distribution may be obtained by applying a threshold to a true distribution

F. Estimation of Directionality

The directionality of the snaps can be estimated from the change in mean of the first component distribution over angle.

An estimate obtained from observed snaps from the bottom from a 4 minute recording (6901 observed snaps, 1158 reflected snaps) is shown in Fig. 11. The estimate was further augmented with observations of surface reflected snaps. These snaps leave the source at a higher angle and provide an additional estimate of source strength at a different angle.

Fig. 11 (a) shows a significant (>2dB) drop in source strength at approximately 20º and 30º degree angles. Fig 11 (b) shows a similar drop at about 18º and a secondary peak followed by a drop at about 31º. The two distinct changes in source strength may be because of two distinct bottom types at the experimental site. This idea is also supported by the fact that divers noticed muddy bottom in some places while sandy bottom in other places during experimental deployments at the same site.

The critical grazing angle of 18º to 20º corresponds to a bottom sound speed of 1577 m/s to 1596 m/s when the sound speed in water is 1500 m/s. This would indicate a bottom type of sand silt clay (c = 1578 m/s) [7], consistent with the muddy bottom observation. The critical grazing angle of 30º to 31º corresponds to a bottom sound speed of 1732 m/s to 1750 m/s. This would indicate a bottom type of fine sand (c = 1740 m/s) [7], consistent with the sandy bottom observation.

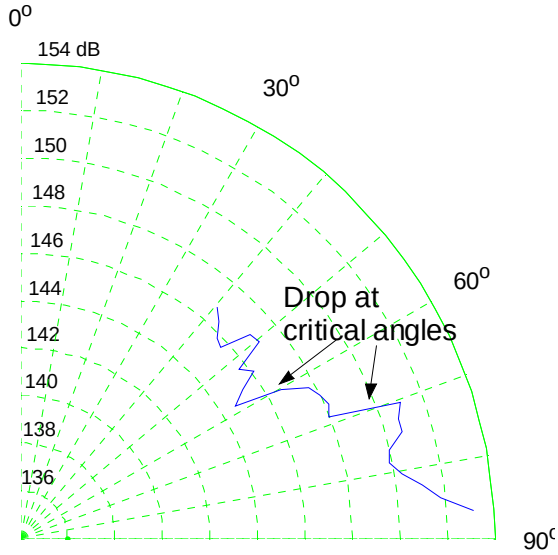

(a) Directionality based on direct arrivals

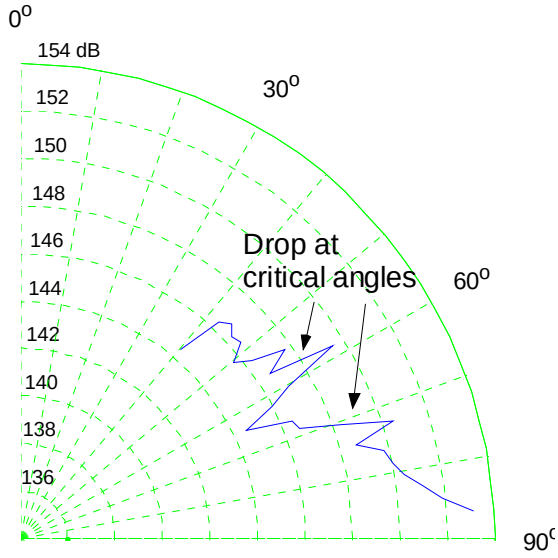

(b) Directionality augmented with surface reflected arrivals

Fig. 11. Estimated directionality on snaps based on a 4 minute dataset

A difference of about 3-4dB is seen between the peak observed source strength at the critical angle and the average observed source strength at higher angles. This suggests an average bubble collapse height off the bottom of about 2-3 cm[c].

V. CONCLUSIONS

Snapping shrimp sounds originate in small bubbles and are therefore omni-directional. However, due to the proximity to the seabed, the interference of the snaps with their bottom reflections gives them directionality. The directionality has been theoretically computed and experimentally verified.

The existence and properties of this directionality may be of interest to systems such as Ambient Noise Imaging where the snaps form the illumination for imaging, as well as for acoustic communications and other signal processing applications where the system performance is limited by the snaps as background noise. Additionally, applications such as simple geo-acoustic inversion may be possible by fitting observed snap probability distributions to models.

The source strength of the snaps seems to obey a log-normal probability distribution, rather than the expected higher entropy normal distribution. This was previously observed for the total energy, but was thought to be an effect of spatial clumping or temporal chorusing.

REFERENCES

[1] Au W.L. & Banks K., "The acoustics of the snapping shrimp Synalpheus parneomeris in Kaneohe Bay", pp41-47, J. Acoust. Soc. Am. **103** (1), 1998.

[2] Verluis M., Schmitz B., Heydt A. & Lohse D., "How Snapping Shrimp Snap: Through Cavitating Bubbles", pp2114-2117. Science **289**, 2000.

[3] Brekhovskikh L. M. & Lysanov Yu. P., "Fundamentals of Ocean Acoustics (2nd edition)", p51. Springer-Verlag, 1990.

[4] Potter J. R. & Chitre M. A., "Statistical models for ambient noise imaging in temperate and tropical waters", 132nd ASA meeting, Honolulu, 1996.

[5] Potter J. R., Lim T. W. & Chitre M. A., "Ambient noise environments in shallow tropical seas and the implications for acoustic sensing", Oceanology International 97, Singapore, 1997.

[6] Potter J. R. & Koay T. B., "Do snapping shrimp chorus in time or cluster in space? Temporal-spatial studies of high-frequency ambient noise in Singapore waters", ECUA 2000, Lyons (France), 2000.

[7] Papadakis P.J. & Piperakis G.S., "An inverse procedure for the reconstruction of a sea bottom consisting of two elastic materials", ECUA 1996, pp. 619-624, Heraklion (Greece), 1996.

[c] Although the average bubble collapse height is about 2-3 cm, the actual value for individual snaps varies significantly. From study of individual snaps, it can be seen that this distance can be as much as 10-20 cm for some snaps.